

# Postmortem Analysis of Sand Grain Crushing From Pile Interface Using X-ray Tomography

Matías Silva I., Gaël Combe, Pierre Foray, Frédéric Flin, Bernard Lesaffre

*Université de Grenoble, 3SR Lab, UMR 5521 Grenoble-INP, UJF-Grenoble 1, CNRS, Grenoble, France*

*CEN, CNRM-GAME UMR 3589, Météo France - CNRS, Grenoble, France*

**Abstract.** Pile foundations of offshore platforms, wind and water turbines are typically subjected to a variety of cyclic loading paths due to their complex environment. While many studies focus on global pile behaviour, the soil-pile interface is explored here by a micromechanical study of the soil layer in contact with the pile surface. This work is devoted to the analysis of frozen post-mortem silica sand samples recovered at the pile interface following installation and cyclic loading tests in a calibration chamber using x-ray tomography. An experimental procedure developed for three dimensional (3D) snow imaging was adapted for the recovery of the in-situ sand samples to preserve their structure during tomography scans. 3D images at a pixel size of  $7\text{ }\mu\text{m}$  were then obtained using a cryogenic cell. Results confirm the presence of a shear band at the pile surface as well as void ratios changes in the direction of the pile's radius.

**Keywords:** X-ray tomography, pile/soil interface, grain crushing, cyclic loading, shearing.

**PACS:** 89.20.Kk, 81.70.Tx.

## INTRODUCTION

Pile foundation is a common concept in the civil engineering domain for supporting heavy structures such as offshore platforms and wind/water turbines in sands. While a lot of effort has been devoted to a better understanding of the global behaviour of displacement piles, the potential effects of particle breakage, shear banding and particle migration in its capacity is not yet very clear.

Colliat (1986) performed several triaxial and direct shear testing in different sands, thus identifying the processes involved in grain crushing mainly related to the stress level developed by the material. Grain crushing is the essential cause of high compressibility of granular media under high confining stress. Belloti et al. (1991) performed a series of laboratory testing and cone penetration tests (CPT) in a calibration chamber device to assess grain crushability in different sands. The crushability threshold appears to occur at the interval of 15 to 20 MPa for silica sands, which seems to be independent of consolidation stress, relative density and an over consolidation ratio.

Although the global capacity of driven piles is relatively simple to obtain, the local distribution of stress along the pile is normally estimated using CPT data or the wave equation analysis (Smith, 1960). Lehané et al. (1993) and Chow (1997) performed a series of field testing on an instrumented cone-ended rigid steel pile in dense sand deposits, measuring through a highly instrumented pile the local stress paths at the pile/soil interface. Their observations

indicate that local shaft failure is controlled by the Mohr-Coulomb criteria. Pile shaft response can be simulated with a constant normal stiffness shear test (CNS) as shown by Mortara et al. (2007).

Analyzing local measurements of a highly instrumented model pile installed on a simulated driven process in a large calibration chamber, Tsuha et al. (2012) concluded that possible local densification and fabric rearrangement may lead to increments in the final shaft capacity after low-level one way axial cyclic loading tests. From similar tests, Yang et al. (2010) performed a series of analyses based on post-mortem sand samples recovered at the pile surface and identified three different zones or layers in the sand clearly modified by the pile installation and following cycling all along the shaft. As the pile tip advances, the crushed material is displaced radially from the pile's axis developing concentric zones with different degrees of particle crushing. At the interface surface, there is a zone of shear band with high crushing rates resulting from the extreme normal and shear stresses developed while the pile is embedded into the sand mass. This zone presents colour changes, high fine content (20%) and adherence to the pile shaft. According to their observations, this zone thickness grows from the pile tip and particularly when the installation is not monotonic, and is augmented by later static and cyclic loading. The second zone presents around 6-8% of fine content with no change in colour. Similar results were obtained by White and Bolton (2004) using PIV (particle image velocimetry) on an aluminum close-ended pile in a plain-strain

model apparatus. There is evidence of particle breakage and soil flow during pile installation around the tip and into the interface zone. The sheared zone presents a thickness of approximately  $2.4D_{50}$ , which agrees with those found by Yang et al. (2010).

Most of the results referred to the mechanism developed at pile surface during installation which treats the subject from a global point of view without dealing with intact samples. The work here presented focuses on an experimental procedure for the recovery of sand samples at the pile interface from calibration chamber testing and their subsequent analysis using X-ray tomography.

## EXPERIMENTAL PROCEDURE

The samples were recovered from the pile's surface of a jacked pile installed in the large calibration chamber of the Laboratory 3SR in Grenoble, France. This chamber consists of a 1.5 m high steel tank of 1.2 m internal diameter. Three rubber membranes installed in the inner part of the chamber allow applying a confinement pressure. An upper membrane applies vertical stress of 150 kPa.

The chamber was filled with industrially prepared silt free, pure, well-distributed, sub-angular Fontainebleau silica sand NE34 using air pluviation technique. With this technique a relative density of 65% can be obtained. The index properties of this sand are presented in Table 1.

**TABLE 1.** Index properties Fontainebleau sand NE34

SiO <sub>2</sub>	G <sub>s</sub>	D <sub>10</sub> mm	D <sub>50</sub> mm	D <sub>60</sub> mm	e <sub>max</sub>	e <sub>min</sub>
99.7	2.65	0.15	0.21	0.23	0.90	0.51

Several pressure sensors were deployed in the sand mass at three levels and at different distances from the pile's axis in order to measure the mobilized radial, vertical and hoop stresses during pile installation and further testing. The model pile used in the tests corresponds to the Mini-ICP pile developed by Imperial College London and described in detail by Jardine et al. (2009). It involves a 36 mm stainless steel cone-ended pile equipped with 3 instrumentation clusters allowing local measurements of radial and shear stresses at the pile's surface. Several load cells installed at the pile's head, clusters and tip measure the axial load distribution.

The pile was embedded to a depth of 0.98 m by non-monotonic jacking with a penetration rate of 2.0 mm/s and jack strokes of 20 mm. The pile head load was reduced to zero at the end of each stroke. After an ageing period of two weeks, the pile was then subjected to 20000 two-way displacement-controlled axial loading cycles.

During installation, the maximum stress at the tip reached between 18 and 20 MPa. High stresses are also mobilized in the soil mass. Figure 1 presents the tip load profile and the radial stresses developed at a distance of  $2R$  from the pile,  $R$  being the pile radius. Figure 2 shows an example of local measurements of radial and shear stresses at the pile's surface during cyclic testing. Local stress paths at the pile surface evidence the development of butterfly wings. The local stress paths engaged phase transformation line showing steps of contractancy and dilatancy during cycling, similar to CNS direct shear tests.

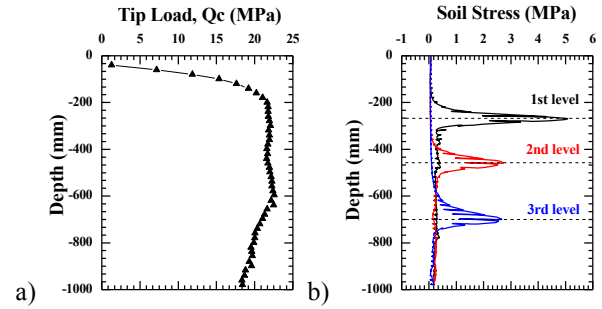


**FIGURE 1.** a)  $Q_c$  profile, b) Radial stress distribution in the sand mass at a distance of  $2R$  from pile axis.

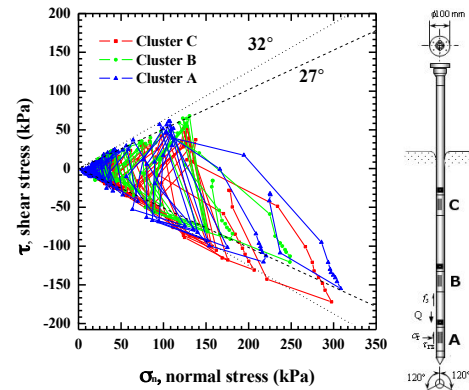


**FIGURE 2.** Example of local stress path during cyclic testing from the instrumented clusters at pile surface.

## SAMPLING

At the end of testing, samples were recovered from around the pile interface, from a depth of 30 cm until the pile's tip. A first solution of water with 40% alcohol content was spilled into the sand to improve its wettability. Pure water was then applied to partially saturate the sand in the vicinity of the pile. By apparent cohesion several samples of partially saturated sand were recovered in a relatively solid state. At the pile surface there was a thin layer of pseudo-cemented sand with a high fine content

characterized by a relative homogeneous grey colour, as presented in Figure 3. According to Yang et al. (2010), the gray colour probably results from intense surface abrasion changing the optical properties of the initial partially polished sand grains.

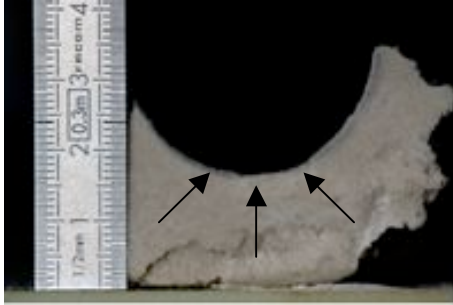


**FIGURE 3.** Examples of recovered samples from pile interface and presence of pseudo-cemented thin sand layer.

These samples were frozen in place immediately after using a small and portable freezer at a temperature of about  $-20^{\circ}\text{C}$ . All the collected samples were then transported to the Snow Research Center of Grenoble (CEN) for further treatment.

To fully saturate the frozen samples, an impregnation with liquid chloronaphthalene took place in the CEN facilities, at an environmental temperature of  $-10^{\circ}\text{C}$ . The processed samples were then refrozen and stored at  $-20^{\circ}\text{C}$ . This operation preserves the samples from sublimation while strengthening them for further machining. The x-ray absorption of chloronaphthalene is similar to the one of water, thus avoiding the presence of an additional material in the image histogram.

Once the samples were in solid state, small cylindrical cores of 15 mm in diameter and 18 mm height were drilled at an environmental temperature of  $-28^{\circ}\text{C}$  to extract the final specimen to be used for x-ray tomography.

## TOMOGRAPHY PROCEDURE

Frozen samples were scanned using x-ray tomography and a cryogenic cell normally used for snow analysis (see e.g. Coleou et al. (2001), Rolland du Roscoat et al. (2011) and Calonne et al. (2012)). For short, the specimens were placed in a refrigerated transparent plexiglas cold cell, mounted on the rotation stage of the tomograph. To maintain the samples in a solid state during scanning, the temperature was maintained at a relative constant value of  $-30^{\circ}\text{C}$ , by using the Peltier device placed at the lower part of the cell. The images were acquired with a pixel size of  $7.282\mu\text{m}$  using x-rays generated at 100 kV of voltage and 100  $\mu\text{A}$  of current. 2400 radiographies with an

average of 6 images per acquisition were recorded in order to reconstruct the 3D model of the sample. Figure 4 presents slices obtained at different depths from the 3D reconstructed volumes.

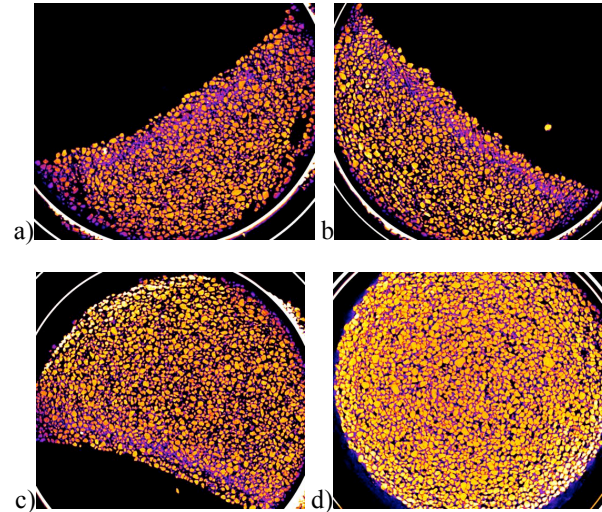


**FIGURE 4.** a) 50 cm, b) 63 cm, c) 81 cm and d) beneath tip.

## MICROSTRUCTURE ANALYSIS

All the analyses were conducted using the free and open source image processing software Fiji. Median filters were applied to all 16 bits images. Figure 5 shows a comparison of two vertical slices of a sample at 50 cm depth: one near the pile surface and one at a distance of 1.8 mm. Fine particles resulting from particle breakage seem to be interlocked between clean grains. Void ratio reduces as the fine content increases. The histogram of the images indicates the presences of mainly 3 materials: chloronaphthalene + water, clean sand grains and crushed sand grains. Though the spatial resolution is relatively high, it is not sufficient to clearly identify individual grains. Fine particles and the edges of pure clean grains present similar absorption properties leading to possible misinterpretation of particle boundaries.

The preliminary results indicate that the thickness of the shear band ranges from approximately  $2,2 D_{50}$  at a depth of 50 cm to  $1,8 D_{50}$  at 81 cm. Shear band thickness and the movement of crushed grains into the sand mass appear to be related to the depth and consequently to the local shearing loading history, as indicated by Yang et al. (2010). The presence of radial flow of fine particles seems to be related to the fluctuation between contractancy and dilatancy stages of cycling. Figure 6 shows the shear bands on two different samples.

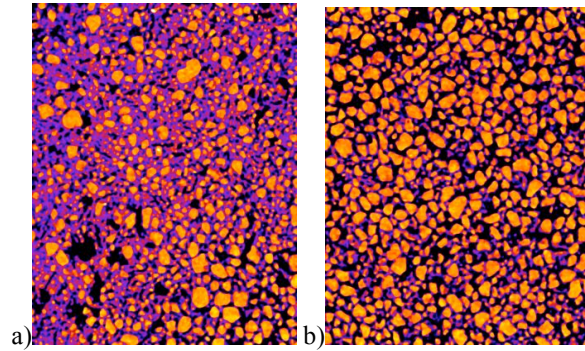


**FIGURE 5.** Vertical slice of a) near pile surface, b) at 1.8 mm from piles axis.

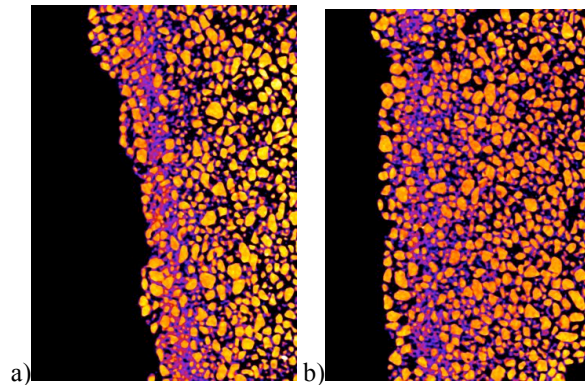


**FIGURE 6.** Profiles of shear band for samples at 50 and 63 cm depth.

## CONCLUSIONS

X-ray tomography is a useful tool for 3D visualization and analysis of grain crushing at the interface of soil-structures. An experimental procedure has been introduced for the sampling and analysis of undisturbed samples recovered from the pile shaft. The presence of a shear band at the surface of the pile indicates high stress concentration and possible shearing during installation and cycling.

## PERSPECTIVES

Further image processing should lead to quantitative measurements of shear band thickness and the evolution of void ratio according to the position from the pile tip and the distance from its axis. These tests will include GA39 silica sand samples ( $D_{50}=0.09$  mm) to evaluate the influence of grain size with respect to pile diameter. Pile installation methods will include a real driven hammered pile unlike current technique consisting on the simulation of driving processes by load cycles.

## ACKNOWLEDGEMENTS

The authors gratefully acknowledge the support of Total France and Meteo France. The authors also extend their thanks to Pascal Charrier, Neige Calonne, Xi Wang et Jacques Roulle for their contributions.

## REFERENCES

1. Colliat-Dangus Jean-Louis (1986). "Comportement des matériaux granulaires sous fortes contraintes - Influence de la nature minéralogique du matériau étudié". Ph.D. Thesis, Université Scientifique et Médicale et l'Institut National Polytechnique de Grenoble.
2. Bellotti R., Fretti C., Ghionna V.N., Pedroni S. (1991). "Compressibility and Crushability of sands at high stresses". Proceedings of the First International Symposium on Calibration Chamber Testing, pp. 79-90.
3. Smith, E.A.L. (1960), "Pile-Driving Analysis by the wave equation", *ASCE Journal of the Geotechnical Engineering Division*, **86**, 35-61.
4. Lehane, B.M., Jardine, R.J., Bond, A.J. & Frank, R. (1993). Mechanisms of shaft friction in sand from instrumented pile tests. *Journal of Geotechnical and Geoenvironmental Engineering*, ASCE, **119** (1), 19-35.
5. Chow, F.C. (1997). "Investigations into displacement pile behaviour for offshore foundations, PhD thesis, Imperial College, University of London.
6. Mortara, G., & Mangiola, A. (2007). "Cyclic shear stress degradation and post-cyclic behaviour from sandsteel interface direct shear tests". *Canadian Geotechnical Journal*, **752**(1978), 739-752.
7. Tsuha, C.H.C., Foray P., Jardine, R.J., Yang, Z.X., Silva M., Rimoy S. (2012). "Behaviour of displacement piles in sand under cyclic axial loading", *Soils and Foundations*, **52**(3), 393-410.
8. Yang, Z. X., Jardine, R. J., Zhu, B. T., Foray, P., & Tsuha, C. H. C. (2010). "Sand grain crushing and interface shearing during displacement pile installation in sand". *Géotechnique*, **60**(6), 469-482.
9. White, D. J., & Bolton, M. D. (2004). "Displacement and strain paths during plane-strain model pile installation in sand". *Géotechnique*, **54**(6), 375-397.
10. Jardine, R., Bitang Z., Foray P., & Dalton, C. (2009). "Experimental Arrangements for Investigation of Soil Stresses Developed around a Displacement Pile". *Soils and Foundations*, **49**(5), 661-673.
11. Coleou, C., Lesaffre, B., Brzoska, J.-B., Ludwig W. & Boller, E. (2001). "Three-dimensional snow images by X-ray microtomography", *Ann. Glaciol.*, **32**, 75-81.
12. Rolland du Roscoat, S., King, A., Philip, A., Reischig, P., Ludwig, W., Flin, F. & Meyssonier, J. (2011). "Analysis of Snow Microstructure by Means of X-Ray Diffraction Contrast Tomography". *Advanced Engineering Materials*, **13**(3), 128-135.
13. Calonne, N., Geindreau, C., Flin, F., Morin, S., Lesaffre, B., Rolland du Roscoat, S. & Charrier, P. (2012). "3-D image-based numerical computations of snow permeability: links to specific surface area, density, and microstructural anisotropy", *The Cryosphere*, **6**, 939-951.